

Spectral characteristics of 2-(4'-*N,N*-dimethylaminophenyl)pyrido[3,4-*d*]imidazole in AOT/*n*-heptane/water reverse micelles

G. Krishnamoorthy, S.K. Dogra *

Department of Chemistry, Indian Institute of Technology, Kanpur, Kanpur 208016, India

Received 20 July 2000; accepted 6 March 2001

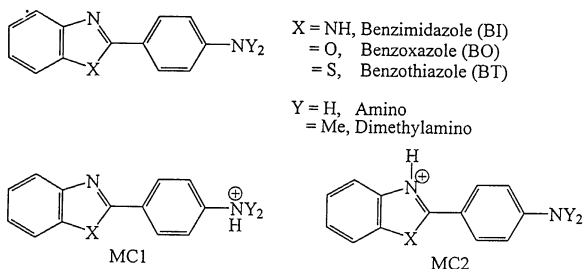
Abstract

Spectral characteristics of 2-(4'-*N,N*-dimethylaminophenyl)pyrido[3,4-*d*]imidazole (DMAPPI) have been studied in AOT/*n*-heptane/water reverse micelles at $w_0 \geq 0$. Absorption, fluorescence excitation and fluorescence spectra have revealed that the monocation (MC) of DMAPPI, protonated at the imidazole nitrogen (MC2) (Scheme 2) is present in the S_0 state at $w_0 = 0$, along with the MC, protonated at pyridine nitrogen (MC3) and only normal emission is observed from both MC2 and MC3. With increase in w_0 (water amount), the equilibrium is shifted towards the MC, protonated at $-NMe_2$ group (MC1) and MC3 in the S_0 state. Biprotic phototautomerism is observed in MC1 to generate MC2 in the S_1 state. The twisted intramolecular charge transfer (TICT) emission replaces the normal emission in MC3. All the MCs are present near the anionic polar head group of AOT in the bound water region. © 2001 Elsevier Science B.V. All rights reserved.

1. Introduction

Acid–base properties of the aromatic compounds, specially heterocyclic molecules, containing one or more than one heteroatoms are always of interest in chemistry and biochemistry [1–8]. It is well known that the acid–base properties of the organic molecules in their excited singlet (S_1) state differ considerably from those in the ground (S_0) state, leading to interesting proton transfer reactions. The utility of such a behaviour in organic

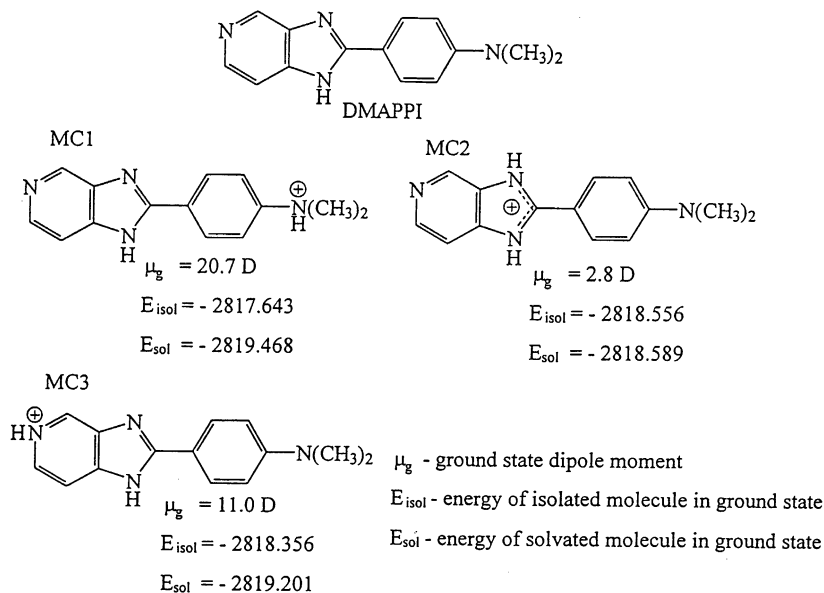
photochemistry has been reviewed recently [9] and the acid–base property of these molecules has been used to probe the characteristics of macromolecules [10–13].



Scheme 1. Structural formulas of the neutral and monocations of aminophenyl or *N,N*-dimethyl derivations of benzazoles.

* Corresponding author. Tel.: +91-512-597163; fax: +91-512-590007.

E-mail address: skdogra@iitk.ac.in (S.K. Dogra).



Scheme 2. Physical parameters of the monocations of DMAPPI, obtained by using AM1 calculations.

Our laboratory has been active nearly for two decades in studying the spectral characteristics of the various prototropic species of heterocycles with either one or two basic centres [14]. The prototropic studies carried out on 2-(4'-aminophenyl, AP) and 2-(4'-*N,N*-dimethylaminophenyl, DMAP) benzimidazole (BI), [15–17] benzoxazole (BO) [18,19] and benzothiazole (BT) [20,17] (Scheme 1) have shown the formation of two kinds of monocations (MCs) in both S_0 and S_1 states, i.e. MC1 is formed by protonating $-\text{NH}_2$ or $-\text{N}(\text{CH}_3)_2$ group and MC2 is obtained by protonating $=\text{N}-$ atom of imidazole ring. The relative populations of MC1 and MC2 depend upon the electronegativity of the benzazole ring and the polarity of the solvents. For example, the major component in the BIs is MC2 and its proportion decreases if BT and BO replace BI in the given order. Further in the polar solvents MC1 (large polar) is more predominant, whereas MC2 (less polar) is predominant in the non-polar solvents.

We have extended this study to DMAPPI (Scheme 2) [21] with the aim that the introduction of one more electronegative atom (N) will increase the electron withdrawing nature of the BI

ring and thus facilitate the formation of TICT state. Further, our earlier studies [15–20] on the MCs of benzazoles have shown that the formation of the TICT state was inhibited by preventing either the charge flow from DMAP group in MC1 or the free rotation of $-\text{NMe}_2$ group in MC2. Hopefully the formation of MC3 will allow the charge flow from $-\text{NMe}_2$ group and thus will increase the fluorescence intensity of the TICT emission from MC3. These studies have shown that in aqueous medium, MC1 and MC3 are formed in the S_0 state. On the other hand, MC2 and MC3 are present in the S_1 state. MC2 is formed in the S_1 state from MC1 by biprotonic phototautomerism. MC3 is emitting from the TICT state and not from the locally excited (LE) state. The relative populations of the MCs depend upon the polarity of the solvents. AM1 semi-empirical quantum mechanical calculations, however, predicted the relative populations of these MCs in the order of $\text{MC2} > \text{MC3} > \text{MC1}$ in the S_0 state under isolated conditions (gas phase or in non-polar solvents) [21] (Scheme 2). We could not establish this prediction, as the ionic species so formed in DMAPPI are insoluble in non-polar solvents. Our study in cyclodextrins (both α - and

β -cyclodextrin) [22] have shown that the relative population of MC3 increases in comparison to MC1 (with respect to aqueous medium). Thus MC1 and MC3 are present in the S_0 state, whereas MC2 and MC3 are present in the S_1 state. In other words, the polarity of the cyclodextrin cavity (similar to that of alcohols) is not non-polar enough for the formation of MC2 in the S_0 state and observation of the emission from the LE state of MC3.

The structure, equilibrium and dynamics of the confined environments and at various interfaces play a crucial role in many biological and natural processes [23,24]. It is known that reverse micelles are interesting models for biological membranes [25]. Reverse micelles are formed by dissolving surfactant molecules in non-polar solvents with non-polar part pointing outward. A remarkable property of the reverse micelles is that it can solubilise large quantities of water to form a spherical pool in the centre of the reverse micelle. The water pool in the reverse micelle has been extensively employed as a reaction medium for enzymolysis [26] and models for water molecules confined in biological systems [27]. As the water/surfactant molar ratio (w_0) increases, besides the hydrodynamic radius of the spherical aqueous micellar core, the microviscosity and polarity of the water pool varies monotonically with w_0 [28,29]. In anionic reverse micelles of AerosolOT (AOT, sodiumbis(2-ethylhexyl)sulphosuccinate) the pK_a value for the acid–base equilibrium increases in comparison to that in aqueous medium because of the acidity of the medium [26]. So the present study on DMAPPI in AOT/*n*-heptane/water reverse micelles was carried out from two angles — (i) whether MC2, as predicted by AM1 calculations, is formed in this medium or not in the S_0 state in the less polar environments of the reverse micelles; and (ii) to see whether any normal emission is observed from the LE state of MC3.

2. Materials and methods

DMAPPI was prepared from 3,4-diaminopyridine and *p*-(*N,N*-dimethylamino)benzoic acid by

the procedure as reported in literature [30]. The compound was purified by repeated crystallisation from aqueous methanol. The purity was checked by TLC and verifying that the fluorescence excitation spectrum in cyclohexane was identical when emission was monitored at different wavelengths. AOT (99%) from sigma was used without further purification. AnalaR grade *n*-heptane (Sisco Research Laboratory) was further purified by the procedure given in the literature [31]. Solvents were checked for spurious fluorescence in the region of fluorescence measurements. To freshly prepared solutions of DMAPPI in AOT reverse micelles in heptane, triply distilled water was added, and solubilised by gentle shaking. The instrument used to record absorption, fluorescence and fluorescence excitation spectra and the procedure used to determine fluorescence quantum yield (ϕ_f) have been described elsewhere [19,21].

3. Results

3.1. Absorption spectrum

Absorption spectrum of DMAPPI has been studied by varying the water amount in AOT concentrations of 0.09, 0.36 and 0.54 M. The relevant data are compiled in Table 1. Fig. 1a depicts the effect of water concentration at different w_0 in 0.54 M AOT. Unlike the absorption spectrum of the neutral DMAPPI in water at pH 9.5 (absorption band maximum; $\lambda_{\max}^{\text{ab}} = 335$ nm), a large red shifted $\lambda_{\max}^{\text{ab}}$ is observed at 364 nm at all the concentrations of AOT in w_0 equal to zero. The $\lambda_{\max}^{\text{ab}}$ is slowly red shifted with the decrease in the absorbance when w_0 is increased. A nice isosbestic point is observed at 370 nm in the absorption spectrum at all the concentrations of AOT studied at varying w_0 (Fig. 1a). The effect of varying AOT concentration is also studied at $w_0 = 0, 3.1, 6.2$ and 18.5. Fig. 1b shows the effect of AOT concentrations at $w_0 = 6.2$. The data at all the w_0 values are compiled in Table 2. For a particular value of w_0 , the $\lambda_{\max}^{\text{ab}}$ is independent of AOT concentrations. At $w_0 = 0$, the absorbance at $\lambda_{\max}^{\text{ab}}$ increases with increase of AOT concentra-

Table 1

Absorption band maxima ($\lambda_{\max}^{\text{ab}}$, nm), absorbance at $\lambda_{\max}^{\text{ab}}$ (A), fluorescence excitation band maxima ($\lambda_{\max}^{\text{ex}}$, nm), fluorescence band maxima ($\lambda_{\max}^{\text{fl}}$, nm) and fluorescence quantum yield (ϕ_{fl}) of MCs of DMAOT/heptane/water reverse micelle at various values of w_0 and at different concentration of AOT along with neat water^a

w_0	[AOT] = 0.09 M				[AOT] = 0.36 M				[AOT] = 0.54 M						
	$\lambda_{\max}^{\text{ab}}$ (A)		$\lambda_{\max}^{\text{ex}}$		$\lambda_{\max}^{\text{fl}}$ (ϕ_{fl})		$\lambda_{\max}^{\text{ab}}$ (A)		$\lambda_{\max}^{\text{ex}}$		$\lambda_{\max}^{\text{fl}}$ (ϕ_{fl})				
	a	b	c	d	a	b	c	d	a	b	c	d			
0	364 (0.173)	356	372 (0.98)	396	450 (0.20)	364 (0.176)	357	373	397 (0.80)	453 (0.24)	364 (0.178)	357	375	400 (0.67)	455 (0.25)
3.1	365 (0.171)	340	373	393 (0.26)	489 (0.11)	365 (0.170)	338	375	394 (0.20)	491 (0.09)	365 (0.166)	337	376	397 (0.19)	490 (0.10)
6.2	366 (0.169)	337	374	397 (0.20)	496 (0.055)	366 (0.168)	330	376	398 (0.15)	498 (0.048)	366 (0.164)	332	377	400 (0.14)	500 (0.11)
9.3	367 (0.168)	335	375	399 (0.15)	500 (0.035)	367 (0.167)	328	377	399 (0.12)	502 (0.027)	367 (0.163)	331	378	401 (0.11)	502 (0.09)
12.4	367 (0.167)	332	376	400 (0.13)	502 (0.026)	367 (0.165)	326	378	402 (0.094)	503 (0.023)	368 (0.162)	328	379	403 (0.088)	503 (0.07)
18.5	368 (0.166)	330	378	403 (0.10)	504 (0.021)	368 (0.164)	325	379	404 (0.077)	504 (0.020)	369 (0.161)	326	379	404 (0.074)	504 (0.06)
24.7	369 (0.165)	327	380	406 (0.08)	505 (0.019)	369 (0.163)	324	380	406 (0.075)	505 (0.017)	369 (0.160)	324	380	406 (0.070)	505 (0.05)
30.9	370 (0.164)	323	380	406 (0.07)	505 (0.018)	370 (0.162)	324	380	406 (0.068)	505 (0.016)	370 (0.157)	324	380	406 (0.066)	505 (0.04)
Neat water MCs (pH 4)											368	310	380	416 (0.003)	525 (0.001)
Neutral (pH 9)											335			415 (0.011)	505 (0.0026)

^a [DMAPPI] = 1×10^{-5} M; a, λ_{em} 380 nm; b, λ_{em} 500 nm; c, λ_{exc} 310 nm; d, λ_{exc} 430 nm.

Table 2

Absorption band maxima ($\lambda_{\max}^{\text{ab}}$, nm), absorbance at $\lambda_{\max}^{\text{ab}}$ (A), fluorescence excitation band maxima ($\lambda_{\max}^{\text{ex}}$, nm), fluorescence band maxima ($\lambda_{\max}^{\text{fl}}$, nm) and fluorescence quantum yield (ϕ_{fl}) of MCs of DMAOT/heptane/water reverse micelle at various concentration of AOT at different w_0 values^a

[AOT]	$w_0 = 0$				$w_0 = 3.1$				$w_0 = 6.2$				$w_0 = 18.5$						
	$\lambda_{\max}^{\text{ab}}$ (A)		$\lambda_{\max}^{\text{ex}}$		$\lambda_{\max}^{\text{fl}}$ (ϕ_{fl})		$\lambda_{\max}^{\text{ab}}$ (A)		$\lambda_{\max}^{\text{ex}}$		$\lambda_{\max}^{\text{fl}}$ (ϕ_{fl})		$\lambda_{\max}^{\text{ab}}$ (A)		$\lambda_{\max}^{\text{ex}}$	$\lambda_{\max}^{\text{fl}}$ (ϕ_{fl})			
	a	b	c	d	a	b	c	d	a	b	c	d	a	b	c				
0.09	364 (0.173)	357	372	396 (0.98)	450 (0.20)	365 (0.171)	339	372	393 (0.26)	488 (0.11)	366 (0.169)	336	374	397 (0.20)	497 (0.055)	368 (0.166)	326	377	403 (0.13)
0.18	364 (0.174)	357	372	397 (0.95)	451 (0.26)	365 (0.170)	337	373	393 (0.24)	488 (0.10)	366 (0.168)	335	375	398 (0.17)	497 (0.053)	368 (0.165)	325	378	404 (0.14)
0.27	364 (0.175)	357	373	397 (0.88)	452 (0.25)	365 (0.168)	336	374	394 (0.22)	488 (0.09)	366 (0.167)	334	376	399 (0.16)	497 (0.050)	368 (0.164)	325	379	405 (0.14)
0.36	364 (0.176)	357	374	398 (0.80)	453 (0.24)	365 (0.167)	334	376	394 (0.20)	489 (0.08)	366 (0.166)	334	377	399 (0.15)	497 (0.048)	368 (0.163)	324	379	406 (0.13)
0.54	364 (0.177)	357	374	401 (0.67)	455 (0.23)	365 (0.166)	334	377	395 (0.18)	489 (0.07)	366 (0.165)	334	378	400 (0.14)	498 (0.047)	368 (0.160)	323	380	407 (0.12)
0.72	364 (0.178)	357	375	403 (0.59)	455 (0.21)	365 (0.165)	333	378	399 (0.16)	489 (0.06)	366 (0.164)	333	379	401 (0.13)	498 (0.046)	368 (0.156)	322	381	407 (0.11)
0.90	364 (0.180)	357	376	406 (0.50)	455 (0.19)	365 (0.164)	333	379	400 (0.14)	489 (0.04)	366 (0.163)	332	380	401 (0.12)	498 (0.044)	368 (0.150)	322	382	408 (0.11)

^a [DMAPPI] = 1×10^{-5} M; a, λ_{em} 380 nm; b, λ_{em} 500 nm; c, λ_{exc} 310 nm; d, λ_{exc} 430 nm.

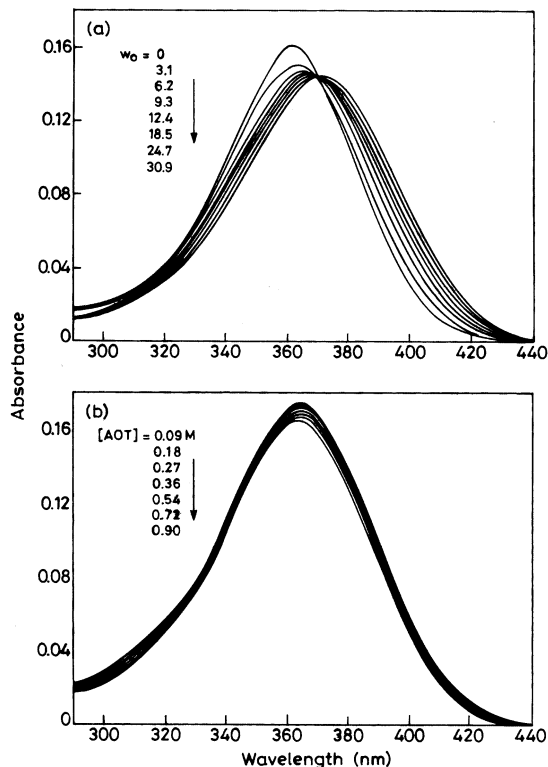


Fig. 1. (a) Absorption spectrum of DMAPPI in 0.54 M AOT at varying concentration of water, $[\text{DMAPPI}] = 0.9 \times 10^{-5}$ M; (b) absorption spectra of DMAPPI at varying concentration of AOT at $w_0 = 6.2$, $[\text{DMAPPI}] = 1 \times 10^{-5}$ M.

tion (Table 2). However, in the presence of a given water content ($w_0 > 0$), the absorbance at the $\lambda_{\text{max}}^{\text{ab}}$ decreases with increase in the AOT concentrations.

3.2. Fluorescence spectrum

Fig. 2 (right hand side panel) depicts the fluorescence spectra of DMAPPI at 0.54 M AOT and $w_0 = 0$ at varying excitation wavelengths (λ_{exc}). At $\lambda_{\text{exc}} = 310$ nm, the fluorescence spectrum is a single band with fluorescence band maximum ($\lambda_{\text{max}}^{\text{fl}}$) at 400 nm. $\lambda_{\text{max}}^{\text{fl}}$ keeps on red shifting with increase in λ_{exc} (i.e. at $\lambda_{\text{exc}} = 430$ nm, $\lambda_{\text{max}}^{\text{fl}} = 455$ nm). Fig. 2 (left-hand side panel) shows the fluorescence excitation spectra of DMAPPI at 0.54 M AOT and $w_0 = 0$ monitored at different emission wavelengths (λ_{em}). The fluorescence excitation band maximum ($\lambda_{\text{max}}^{\text{exc}}$) also keeps on red shifting with increase in λ_{em} . The $\lambda_{\text{max}}^{\text{fl}}$, full width at half the maximum height (FWHM) and ϕ_{fl} at each λ_{exc} , as well as the $\lambda_{\text{max}}^{\text{exc}}$ and FWHM at each λ_{em} are compiled in Table 3. The ϕ_{fl} is maximum at $\lambda_{\text{exc}} = 310$ nm, and keeps on decreasing with increase of λ_{exc} . $\lambda_{\text{max}}^{\text{fl}}$ keeps on red shifting under the similar conditions. FWHM of the fluorescence spectrum first increases up to $\lambda_{\text{exc}} = 370$ nm, but then decreases sharply at $\lambda_{\text{exc}} > 370$ nm. Similarly,

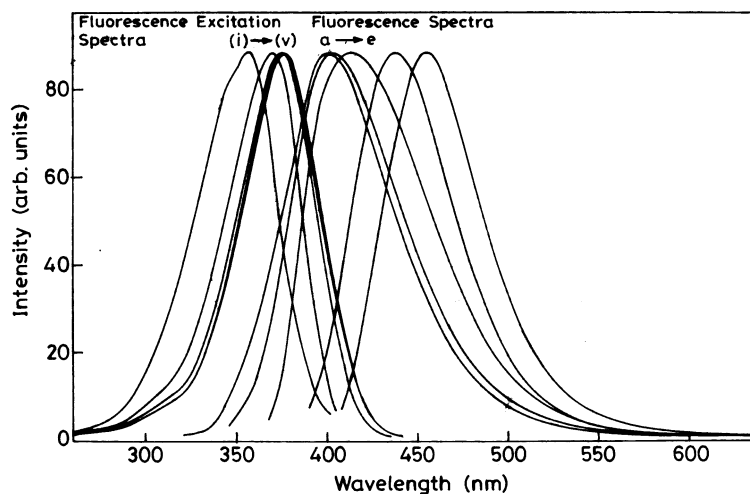


Fig. 2. Left hand side (\leftarrow), fluorescence excitation spectra of DMAPPI at λ_{em} (nm): (i) 380; (ii) 410; (iii) 440; (iv) 470; (v) 500; right hand side (\rightarrow), fluorescence spectra of DMAPPI at λ_{exc} (nm): (a) 310; (b) 340; (c) 370; (d) 400; and (e) 430 in 0.54 M AOT in heptane at $w_0 = 0$. $[\text{DMAPPI}] = 1 \times 10^{-5}$ M.

Table 3

Fluorescence excitation band maxima ($\lambda_{\text{max}}^{\text{ex}}$) and FWHM (cm^{-1}) at different λ_{em} (nm), and fluorescence band maxima ($\lambda_{\text{max}}^{\text{fl}}$, nm), fluorescence quantum yield (ϕ_{fl}) and FWHM at each λ_{exc} of DMAPPI in 0.54 M AOT at $w_0 = 0$

Excitation spectra			Fluorescence spectra			
λ_{em}	$\lambda_{\text{max}}^{\text{ex}}$	FWHM	λ_{exc}	$\lambda_{\text{max}}^{\text{fl}}$	ϕ_{fl}	FWHM
380	357	4290	310	400	0.67	4240
410	370	3600	340	404	0.32	4300
440	373	3630	370	413	0.28	4420
470	374	3650	400	438	0.27	3180
500	375	3610	430	455	0.23	3020

the $\lambda_{\text{max}}^{\text{exc}}$ is red shifted with the increase in the λ_{em} , whereas the FWHM of the excitation spectrum is maximum at $\lambda_{\text{em}} = 380$ nm and nearly remains unchanged at other λ_{em} .

Fig. 3 shows the fluorescence spectra (right hand panel) at $\lambda_{\text{exc}} = 310$ nm and the fluorescence excitation spectra (left hand panel) at $\lambda_{\text{em}} = 380$ nm as a function of w_0 . The fluorescence spectrum and fluorescence excitation spectrum under similar conditions in pure water at pH 4.0 is also shown in Fig. 3 for comparison. Unlike in AOT at $w_0 = 0$, dual emission is observed with the addition of water to AOT. For initial addition of

water ($w_0 = 3.1$), $\lambda_{\text{max}}^{\text{fl}}$ of the short wavelength (SW) band is slightly blue shifted. On further addition of water, $\lambda_{\text{max}}^{\text{fl}}$ of SW band is red shifted up to $w_0 = 24.7$ and no change in $\lambda_{\text{max}}^{\text{fl}}$ is noticed with further increase of w_0 . On the other hand, the $\lambda_{\text{max}}^{\text{exc}}$ of DMAPPI at 0.54 M AOT and $\lambda_{\text{em}} = 380$ nm keep on blue shifting with increase in w_0 (357 nm at $w_0 = 0$ to 324 nm at $w_0 = 24.7$).

Fig. 4 depicts the fluorescence spectra (right panel) at $\lambda_{\text{exc}} = 430$ nm and the fluorescence excitation spectra (left panel) at $\lambda_{\text{em}} = 500$ nm of DMAPPI in 0.54 M AOT as a function of w_0 . The similar spectra of DMAPPI in pure water and at the same λ_{exc} and λ_{em} at pH 4.0 are also shown in Fig. 4 for comparison purposes. For initial addition of water ($w_0 = 3.1$) the fluorescence spectrum is largely red shifted from 455 nm (at $w_0 = 0$) to 490 nm and then slowly to 500 nm with further increase in water (at $w_0 = 24.7$). At $w_0 > 24.7$, no further increase in $\lambda_{\text{max}}^{\text{fl}}$ is observed. Unlike the emission spectra, the red shift observed in the fluorescence excitation spectra at $\lambda_{\text{em}} = 500$ nm is small for initial addition of water from 375 to 376 nm (at $w_0 = 3.1$). On the other hand, $\lambda_{\text{max}}^{\text{exc}}$ is slowly red shifted up to $w_0 = 24.7$ and no further change is noticed at $w_0 > 24.7$. All the relevant data at various concentrations of AOT are compiled in Table 1. ϕ_{fl} of both the bands of

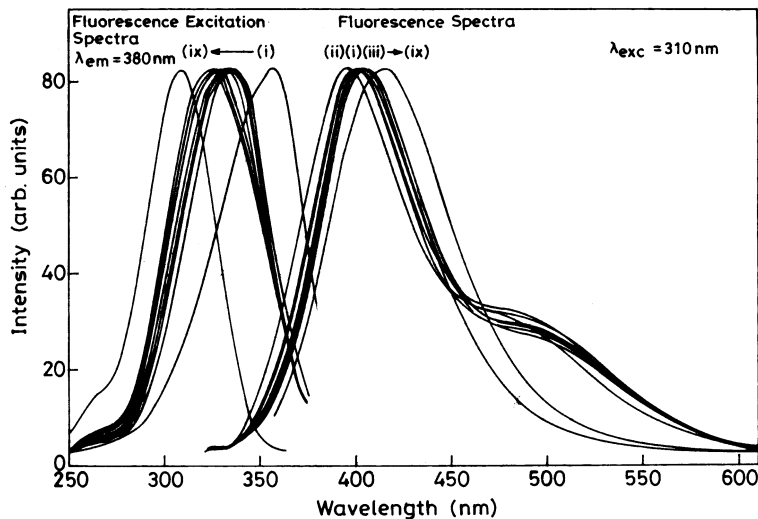


Fig. 3. Fluorescence excitation spectra ($\lambda_{\text{em}} = 380$ nm, left hand side panel) and fluorescence spectra ($\lambda_{\text{exc}} = 310$ nm, right hand side panel) of DMAPPI in 0.54 M AOT as function of w_0 . w_0 : (i) 0; (ii) 3.1; (iii) 6.2; (iv) 9.3; (v) 12.4; (vi) 18.5; (vii) 24.7; (viii) 30.9; (ix) neat water at pH 4.0.

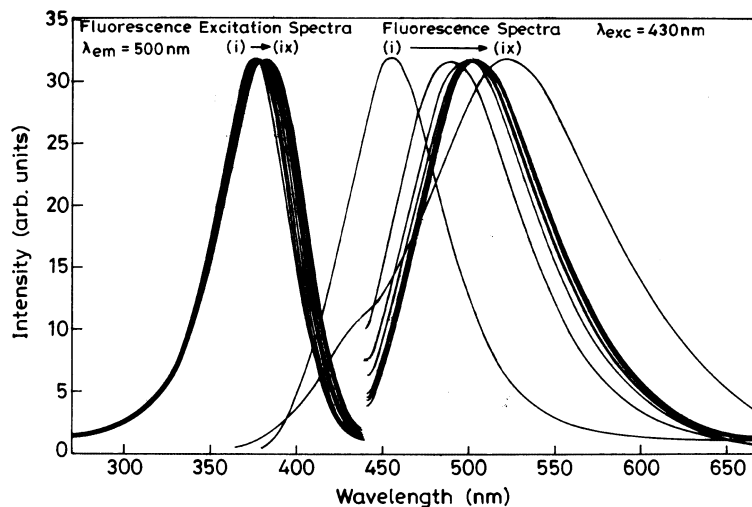


Fig. 4. Fluorescence excitation spectra ($\lambda_{em} = 500$ nm, left hand side panel) and fluorescence spectra ($\lambda_{exc} = 430$ nm, right hand side panel) of DMAPPI in 0.54 AOT as function of w_0 . w_0 : (i) 0; (ii) 3.1; (iii) 6.2; (iv) 9.3; (v) 12.4; (vi) 18.5; (vii) 24.7; (viii) 30.9; (ix) neat water at pH 4.0 (in neat water the shoulder at 440 nm is due to normal emission of MC2 rather than that of MC3 as the corresponding fluorescence excitation spectra give the 310-nm band and not the 380 nm).

DMAPPI under above conditions as a function of w_0 is plotted in Fig. 5. ϕ_{fl} of both the bands decreases sharply with the initial increase of w_0 but decreases slowly with further increase in w_0 .

Fluorescence and fluorescence excitation spectra of DMAPPI were also studied as a function of AOT concentration at $w_0 = 0, 3.1, 6.2$ and 18.5 . The relevant data are compiled in Table 2. At $w_0 = 0$, no change is observed in the λ_{max}^{exc} at $\lambda_{em} = 380$ nm with increase in AOT concentration. However, at $\lambda_{em} = 500$ nm, the fluorescence excitation spectra and fluorescence spectra at both excitation (310 and 430 nm) are red shifted with increase in AOT concentrations. On the other hand, at $w_0 > 0$, the λ_{max}^{exc} are blue and red shifted when monitored at 380 and 500 nm emissions, respectively, with increase of AOT concentration at each w_0 value. Fig. 6a and b shows the plot of ϕ_{fl} of the fluorescence bands at λ_{exc} 310 and 430 nm, respectively, as a function of AOT concentration and at different w_0 values. At $\lambda_{exc} = 310$ nm, the ϕ_{fl} of the SW emission decreases with increase of AOT concentration at each w_0 . But the decrease in ϕ_{fl} of the SW emission as a function of AOT concentration at $w_0 = 0$ is faster than that at

$w_0 > 0$. At $\lambda_{exc} = 430$ nm and at $w_0 = 0$, the ϕ_{fl} of the long wavelength (LW) emission band first increases up to 0.18 M AOT concentration and then decreases with further increase of AOT concentration. However, at $w_0 > 0$, similar to the SW emission band, the ϕ_{fl} of the LW emission decreases under similar environments. Finally, the fluorescence excitation and fluorescence band maximum of the MCs of DMAPPI at the extreme water content in 0.09 M AOT are summarised in Table 4.

Table 4

Fluorescence excitation band maxim (λ_{max}^{exc}) and fluorescence band maxim (λ_{max}^{fl} , nm) of the MCs of DMAPPI in different w_0 values in reverse micelles^a

w_0	MC1		MC1		MC1	
	λ_{max}^{exc}	λ_{max}^{fl}	λ_{max}^{exc}	λ_{max}^{fl}	λ_{max}^{exc}	λ_{max}^{fl}
0	—	—	356	396	372	450
30.9	323	—	—	406	380	505
Neat water	310	—	—	416	380	525

^a [AOT] = 0.09 M.

4. Discussion

4.1. AOT/*n*-heptane reverse micelle

Our earlier study [21] in pure water has confirmed that the $\lambda_{\text{max}}^{\text{exc}}$ at 310 and 380 nm are due to MC1 and MC3, respectively. The emission band at 525 nm is attributed to the TICT emission from MC3 and the 416 nm emission band is due to the normal emission of MC2, formed in the S_1 state from MC1 by the biprotonic phototautomerism, as the $-\text{NHMe}_2^+$ group becomes stronger acid in the S_1 state and dissociates to protonate =N-atom of imidazole ring, which becomes stronger base on excitation.

Before we assign the spectral characteristics to the various species of DMAPPI in AOT reverse

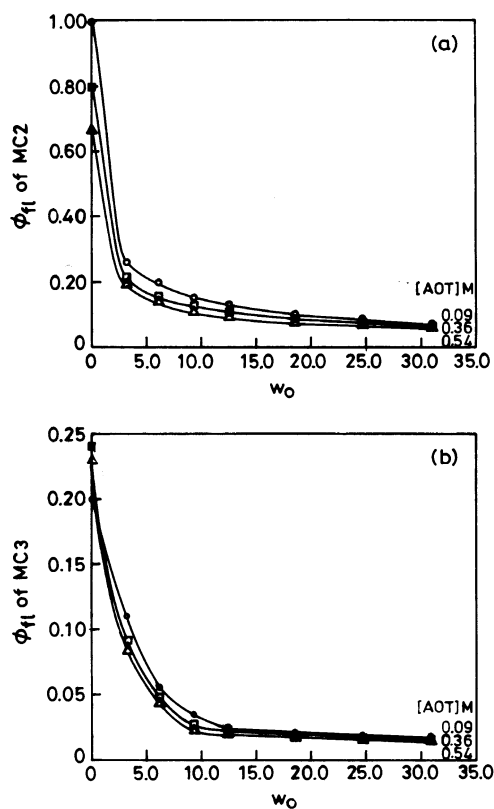


Fig. 5. Plot of fluorescence quantum yields of (a) MC2 ($\lambda_{\text{exc}} = 310$ nm) and (b) MC3 ($\lambda_{\text{exc}} = 430$ nm) as a function of w_0 at different AOT concentration.

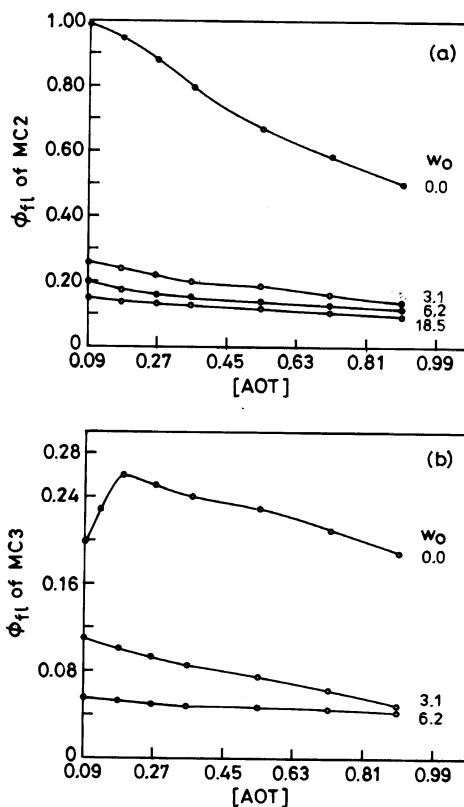


Fig. 6. Plot of fluorescence quantum yields of (a) MC2 ($\lambda_{\text{exc}} = 310$ nm); and (b) MC3 ($\lambda_{\text{exc}} = 430$ nm) as a function of AOT concentration at different w_0 values.

micelles, it may be mentioned that the interfacial region of the AOT reverse micelle even at $w_0 = 0$ is acidic enough to protonate the various basic groups of DMAPPI. This is because the spectral characteristics of DMAPPI so observed in AOT reverse micelles and at $w_0 = 0$ are large red shifted in comparison to the neutral species [32] and are close to those of the MCs of DMAPPI in water [21]. The $\lambda_{\text{max}}^{\text{exc}}$ at ~ 375 nm is close to that of MC3 in water (380 nm). So it can be assigned to MC3. Small blue shift observed in the fluorescence excitation spectra of MC3 is due to the presence of species in less polar environments of the reverse micelles. On increasing the amount of water in AOT reverse micelles (i.e. increasing the polarity), the $\lambda_{\text{max}}^{\text{exc}}$ is red shifted and matches with

the value observed in pure water. This observation substantiates our above assignment. As the emission at 455 nm in AOT at $w_0 = 0$ arises from the ~ 375 nm fluorescence excitation band, it can be assigned to MC3. This behaviour is very different from that observed in pure aqueous medium in the sense that the emission from the LE state of MC3 was absent in the pure aqueous medium. In other words, the emission at 455 nm of the MC3, which is largely blue shifted compared with that in neat water, could be due to the emission from the LE state rather than from the TICT state. To confirm this, the emission spectrum of the MC3 of DMAPPI in acidified methanol at $\lambda_{\text{exc}} = 430$ nm was recorded at liquid nitrogen temperature. At this temperature, the free rotation of $-\text{NMe}_2$ group is frozen, preventing the twisting of $-\text{NMe}_2$ group and thus the emission is only observed from the LE State. The emission band maximum thus obtained at 455 nm in the acidified methanol at liquid nitrogen temperature (not shown) agrees with the value obtained in AOT reverse micelles at $w_0 = 0$.

The other emission band at 400 nm in AOT at $w_0 = 0$ behaves similar to that of 416 nm in pure water and thus can be assigned to MC2. The blue shift observed in the $\lambda_{\text{max}}^{\text{f}}$ can be explained in the same manner as done for the MC3. But the corresponding $\lambda_{\text{max}}^{\text{exc}}$ does not resemble with that noticed in pure aqueous medium (i.e. 310 nm). It is large red shifted as compared with 310 nm band and the red shift observed at $w_0 = 0$ (~ 350 nm) is even larger than that of the neutral DMAPPI (~ 335 nm) in homogeneous solvents [32]. It can thus be assigned to MC2 in the S_0 state. The above assignment is further substantiated from the following argument. It is well established [33–36] that if $\pi \rightarrow \pi^*$ is the lowest energy transition, the protonation at the pyridine = N– atom leads to large red shift and the protonation at the imidazole = N– atom to small red shift in the absorption spectrum of the neutral species. Thus from the above results, it may be concluded that (i) the absorption spectra of DMAPPI in AOT at $w_0 = 0$ is due to the combination of the absorption spectra of MC2 and MC3; and (ii) the emissions observed at 400 nm and at 455 nm are from the LE states of the MC2 and MC3, respectively.

(iii) The above conclusions obviously hold only if one can visualise a reverse micelle at $w_0 = 0$ and a trace of water is present. It has been shown that this small trace of water may be from hydrocarbons or from AOT. The AOT micelle consists of small droplets containing water, the surfactant and counterions in an oil continuum. In other words the presence of water in trace amounts, was in fact, suggested to be a prerequisite for surfactant aggregation in organic solvents [37–41]. Since only one pK_a value (6.75) is observed for the equilibrium between different MCs (MC1 and MC3) and neutral species of DMAPPI in neat water [21], the presence of even trace amount of water will protonate the basic centres of DMAPPI due to acidity of AOT reverse micelle [26]. (iv) Absence of any isosbestic point over the entire range of surfactant used (0.0–0.9 M) suggests that no specific interactions seem to occur with the surfactant molecule in the ground state. In other words only dipole–dipole interactions seem to occur between the probe molecule and surfactant. This is supported by the absence of the TICT emission band of MC3 at $w_0 = 0$. (v) Lastly it may be pointed out that the positive part of MC2 or MC3 (i.e. pyrido imidazole, PI ring) is present near the polar head group of the surfactant. This seems to be consistent with the structure of the AOT molecule, i.e. AOT is a diester derivative of succinic acid with two long hydrocarbon chains from the ester group. The sulphonate (SO_3^-) group is in the α -position of one of the ester group and in the β -position of the other so as to form the negative polar head group of the surfactant molecule. Further, the sulphonate and ester groups remain within the skeleton of the succinic acid part of the molecule [42–44].

4.2. AOT/*n*-heptane/water reverse micelle

The presence of an isosbestic point at 370 nm in the absorption spectra on varying water amount (Fig. 1a) suggests the presence of equilibrium. We have tried to use the Benesi–Hildebrand equation [45] for 1:1, 1:2 and 1:3 complexes between the MC of DMAPPI and water molecules. In each case, the double reciprocal plot between $1/[I - I_0]$ (where I_0 and I are absorbances at $w_0 = 0$ and

> 0) and $1/[\text{H}_2\text{O}]^n$ (taking different values of n) is not linear (not shown). This suggests that different kind of solvated MCs of DMAPPI are in equilibrium. Presence of different kind of solvated molecules either in neutral or MCs have been shown earlier also by noting the red shifts observed in the fluorescence excitation spectra with increase in λ_{em} [21,32]. This behaviour is different from that observed by Belletete et al. [46] for 2-(4'-*N,N*-dimethylaminophenyl)

-3,3-dimethyl-3H-indole and water molecule in AOT, as the latter molecule contains only one basic centre compared with three in the present case. Thus they found out that the probe molecule and the water molecule form a 1:1 association complex. Further based on their temperature dependent study, they have shown that the complex formed is a hydrogen bonded complex between the probe and the water molecules. Although we have not carried out a similar study, based on the following results (i.e. small red shifts observed in the $\lambda_{\text{max}}^{\text{ab}}$, red shift observed in the 400 nm fluorescence band and the TICT band, see below) a similar hydrogen bonded complexes containing different kinds of stoichiometric complexes of probe with water molecules can also be suggested in our case.

Two points are worth mentioning about the results observed when water is added to AOT/*n*-heptane system. The first, a large blue shift is observed in the fluorescence excitation spectra monitored at 380 nm and the second a large red shift is observed in the fluorescence spectra observed at $\lambda_{\text{exc}} = 430$ nm. As pointed out earlier [21] (Scheme 2) the MC1 is highly polar ($\mu_{\text{g}} = 20.7$ D) and the MC2 is the least ($\mu_{\text{g}} = 2.8$ D). It is also shown by Belletete et al. [29] that at $w_0 = 0$, the effective dielectric constant at the interface of the AOT reverse micelles is 2.2 and it increases with increase in the water amount. Thus at $w_0 = 0$, both MC2 and MC3 are present and are confirmed by absorption, fluorescence excitation and fluorescence spectra. With the increase in the water content, the least polar MC2 will be transformed into MC1 or MC3. As shown earlier, the MC2 in neat water is formed in the S_1 state from the MC1, similar phenomenon is also responsible for the formation of MC2 from MC1 in the

reverse micelles and this process is also quite fast in these microenvironments. The decrease in the fluorescence quantum yield of MC2 on increasing w_0 is due to the solvent induced quenching as the magnitude of fluorescence quantum yield decreases with increase of water content.

The large red shift in the fluorescence spectrum of MC3, even at the smallest amount of water ($w_0 = 3.1$) has been assigned to the TICT state of MC3 and can be explained as follows. In neutral DMAPPI, [32] the TICT emission is only observed in polar/protic solvents suggesting that the hydrogen bonding plays the major role in the TICT emission. It has also been shown earlier that the hydrogen bonding of the solvents with PI ring tends the PI ring to be more planar with the benzene ring, thereby facilitating the charge flow from dimethylaminophenyl ring to the PI ring. Thus it was suggested that it was the twisting of the $-\text{NMe}_2$ group and planarity of the PI ring with benzene ring leads to the TICT emission. In MC3, the electron withdrawing nature of the PI ring increases due to the protonation and addition of water leads the PI ring and benzene ring to be more planar. This will lead to greater charge flow from $-\text{NMe}_2$ group to PI ring and thus enhancement of TICT emission at the expense of normal emission. Further addition of water will also quench the normal emission as observed in neat water. As observed earlier, formation of TICT state is an excited state phenomenon and has the same ground state precursor as for the LE emission. A small red shift (~ 6 nm) observed in the fluorescence excitation spectra when monitored at 500 nm is due to the solvation of the MC3 of DMAPPI to different extent as suggested earlier.

All the MCs are present in the bound water region near the polar head group of the surfactants, which is less polar than the free water in the entrapped pool. This conclusion is based on the following arguments. (i) The ϕ_{n} of both the emission bands decrease very sharply on addition of small amount of water (Fig. 5) and then remains nearly independent with further addition of water. Similar sharp decrease in ϕ_{n} is also observed for 4-aminonaphthalimide in AOT/*n*-heptane/water [47] and 8-anilinonaphthalene sulphonic acid in TX-100/hexanol/water in cyclohexane [48] reverse

micelles, where the fluorophore is present in the entrapped water pool. Similar results are also observed by us for the MCs of DMAPPI in TX-100/hexanol/water in cyclohexane reverse micelle and the MCs are present in the water pool [49]. (ii) The changes observed on varying AOT concentration (Fig. 6) are less in comparison to those observed on addition of water (Fig. 5). Small changes in the ϕ_{fl} are due to small variation of the polarity in the micellar interface due the change in AOT concentration [29]. (iii) Our earlier studies of DMAPPI in cyclodextrins [22] have shown that besides the hydrogen bonding of the solvents with the electron acceptor group (PI ring), the dipole–dipole interactions of the solvent molecules with electron donor group ($-NMe_2$) also plays a role in the stabilisation of the TICT state. Even at $w_0 = 30.9$, the fluorescence maximum of MC3 is 20 nm blue shifted and ϕ_{fl} is ~ 21 times that observed in neat water. (iv) Similarly at $w_0 = 30.9$, the fluorescence maximum of MC2 is blue shifted by 10 nm and ϕ_{fl} is ~ 24 times larger than those observed in neat water.

5. Conclusions

The above study reveals that in the AOT/*n*-heptane reverse micelle, a trace amount of water is present even at $w_0 = 0$ and this is confirmed by the presence of the MCs of DMAPPI rather than the neutral species. MC2 is formed in the S_0 state along with MC3 at $w_0 = 0$, as predicted by the theoretical calculations. The normal emission is only observed from MC3 when excited at 430 nm, suggesting that the amount of water for hydrogen bonding is nearly negligible and MC1 is completely absent. On increasing the water amount, the equilibrium is shifted towards MC1 and MC3 in the S_0 state. However, in the S_1 state, similar to other medium, MC2 is present with MC3. In other words, biprotonic phototautomerism is observed in AOT/*n*-heptane/water reverse micelles during the lifetime of MC1. The normal emission from MC3 is quenched and the TICT emission is noticed with increase of water content. All the MCs are present near the polar head group in the bound water region.

Acknowledgements

The authors are thankful to the Department of Science and Technology, New Delhi, for the financial support to the project no. SP/SI/H-39/96.

References

- [1] J.F. Ireland, P.A.H. Wyatt, *Adv. Phys. Org. Chem.* 12 (1976) 131.
- [2] S.G. Schulman, in: E.L. Wehry (Ed.), *Modern Fluorescence Spectroscopy*, Plenum Press, New York, 1976.
- [3] L.G. Arnaut, S.J. Formosinho, *J. Photochem. Photobiol. A Chem.* 75 (1993) 21.
- [4] M. Novo, M. Mosquera, F.R. Prieto, *J. Phys. Chem.* 99 (1995) 14726.
- [5] S.M. Ormson, R.G. Brown, *Prog. React. Kinet.* 19 (1994) 211.
- [6] J.K. Dey, S.K. Dogra, *J. Photochem. Photobiol. A Chem.* 66 (1992) 15.
- [7] S. Santra, S.K. Dogra, *J. Mol. Struct.* 478 (1999) 478.
- [8] J.K. Dey, J.L. Haynes III, I.M. Wener, *J. Phys. Chem. A* 101 (1997) 4872.
- [9] P. Wan, D. Shukla, *Chem. Rev.* 93 (1993) 571.
- [10] S. Nigam, R.S. Srapal, S.K. Dogra, *J. Coll. Interf. Sci.* 163 (1994) 152.1.
- [11] S. Pandey, R.S. Srapal, S.K. Dogra, *J. Coll. Interf. Sci.* 172 (1995) 407.
- [12] S.K. Saha, P. Tiwari, S.K. Dogra, *J. Phys. Chem.* 98 (1994) 3638.
- [13] S.K. Das, S.K. Dogra, *J. Chem. Soc. Faraday Trans. I* 94 (1998) 139.
- [14] S.K. Dogra, *Proc. Indian Acad. Sci.* 104 (1992) 635.
- [15] A.K. Mishra, S.K. Dogra, *Bull. Chem. Soc. Jpn.* 58 (1985) 3587.
- [16] G. Krishnamoorthy, S.K. Dogra, *J. Photochem. Photobiol. A Chem.* 123 (1999) 109.
- [17] J.K. Dey, S.K. Dogra, *J. Phys. Chem.* 98 (1994) 3698.
- [18] J.K. Dey, S.K. Dogra, *Chem. Phys.* 143 (1990) 97.
- [19] G. Krishnamoorthy, S.K. Dogra, *Chem. Phys.* 243 (1999) 45.
- [20] J.K. Dey, S.K. Dogra, *Bull. Chem. Soc. Jpn.* 64 (1991) 3142.
- [21] G. Krishnamoorthy, S.K. Dogra, *J. Org. Chem.* 64 (1999) 6566.
- [22] G. Krishnamoorthy, S.K. Dogra, *J. Phys. Chem. A* 104 (2000) 2542.
- [23] K.B. Einsenthal, *Chem. Rev.* 96 (1996) 1343.
- [24] S.B. Zhu, S. Singh, G.W. Robinson, *Adv. Chem. Phys.* 85 (1994) 627.
- [25] J.H. Fendler, *Membrane Mimetic Chemistry*, Wiley, New York, 1982, p. 48.

- [26] P.L. Luisi, M. Giomini, M.P. Pileni, R.H. Robinson, *Biochim. Biophys. Acta* 947 (1988) 209.
- [27] D.L. Sackett, J.R. Knutson, J. Wolff, *J. Biol. Chem.* 265 (1990) 14899.
- [28] M. Hasegawa, T. Sugimura, Y. Suzaki, Y. Shindo, *J. Phys. Chem.* 98 (1994) 2124.
- [29] M. Belletete, M. Lachapelle, G. Durocher, *J. Phys. Chem.* 94 (1990) 5337.
- [30] R.W. Middleton, D.G. Wibberly, *J. Heterocyclic Chem.* 17 (1980) 1757.
- [31] M.J. Riddick, W. Bunger, *Organic Solvents*, Wiley, New York, 1970.
- [32] G. Krishnamoorthy, S.K. Dogra, *Spectrochim. Acta A* 55 (1999) 6566.
- [33] P.C. Tway, L.J. Cline Love, *J. Phys. Chem.* 86 (1982) 5227.
- [34] M. Krishnamuthy, P. Phaniraj, S.K. Dogra, *J. Chem. Soc. Perkin Trans. II* (1986) 1917.
- [35] H.K. Sinha, S.K. Dogra, *J. Chem. Soc. Perkin Trans. II* (1987) 1465.
- [36] U. Reimann, F. Bergmann, D. Litchenberg, Z. Neiman, *J. Chem. Soc., Perkin Trans. I* (1973) 793.
- [37] H.F. Eicke, H. Christen, *Helv. Chim. Acta* 61 (1978) 2258.
- [38] B. Djermouni, H.J. Ache, *J. Phys. Chem.* 83 (1979) 2476.
- [39] U. Hermann, Z.A. Schely, *J. Am. Chem. Soc.* 101 (1979) 2665.
- [40] J. Rouviere, J.M. Couret, M. Lindhermer, J.L. Deyardin, R. Marroyn, *J. Chim. Phys.* 76 (1979) 289.
- [41] M.A. Rodgers, P.C. Lee, *J. Phys. Chem.* 88 (1984) 3480.
- [42] T.K. Jain, M. Varshney, A. Maitra, *J. Phys. Chem.* 93 (1989) 7409.
- [43] A.N. Maitra, H.F. Eicke, *J. Phys. Chem.* 85 (1981) 2687.
- [44] A.N. Maitra, *J. Phys. Chem.* 88 (1984) 5122.
- [45] D.W. Cho, Y.H. Kim, S.G. Kang, M. Yoon, D.J. Kim, *J. Chem. Soc. Faraday Trans.* 92 (1996) 29.
- [46] M. Belletete, M. Lachapelle, G. Durocher, *J. Phys. Chem.* 94 (1990) 7642.
- [47] S. Das, A. Datta, K. Bhattacharyya, *J. Phys. Chem. A* 101 (1997) 3299.
- [48] C. Kumar, D. Balasubramanian, *J. Coll. Interf. Sci.* 74 (1980) 64.
- [49] G. Krishnamoorthy, S.K. Dogra, *J. Coll. Interf. Sci.* 228 (2000) 335.